Research Journal of Applied Sciences, Engineering and Technology 4(22): 4646-4655, 2012
ISSN: 2040-7467

Submitted: March 19, 2012 Accepted: April 20, 2012 Published: November 15, 2012

Electric Equivalent Models of Intrinsic Recombination Velocities of a Bifacial Silicon Solar Cell under Frequency Modulation and Magnetic Field Effect

[1]Nd. Thiam, [1]A. Diao, [1]M. Ndiaye, [1]A. Dieng, [1]A. Thiam, [2]M. Sarr, [3]A.S. Maiga and [1]G. Sissoko
[1]Laboratory of Semiconductors and Scharolar Energy, Physics Department,
Faculty of Science and Technology, University Cheikh Anta Diop, Dakar, Senegal
[2]UFR/SET, University Thies, Thies, Senegal
[3]Section de Physique Appliquée, UFR/SAT, Université Gaston Berger, Sénégal

Abstract: In this study, we present a theoretical study of the photogenerated charge carriers in the base of an illuminated n^+-p-p^+ crystalline silicon solar cell under an external magnetic field. By solving the charge carriers' continuity equation, the dependence of diffusion coefficient and the photocurrent density on the frequency modulation and magnetic field, is studied. Hence, the study of intrinsic recombination velocities at the junction Sfo1 and rear side Sbo1 of the solar cell, leads to electric equivalent models.

Keywords: Frequency modulation, magnetic field, recombination velocity, silicon solar cell

INTRODUCTION

The determination of solar cell phenomenological and electric parameters is necessary to have better energy conversion efficiency (Wang *et al*., 1990; Hübner *et al*., 2001). Several studies were carried on an n+-p-p+ type solar cell (Hübner *et al*., 2001; Daniel *et al*., 1988) in order to optimize the photovoltaic energy conversion efficiency. In this study, a study of a silicon solar cell under polychromatic light illumination in frequency modulation and external magnetic field effect is proposed. From the minority carriers' density in the base, we deduce the photocurrent density witch leads to the determination of the intrinsic recombination velocities at the junction Sfo1 and the back side Sbo1. Complex expressions of Sfo1 and Sbo1 are obtained. Their real and imaginary parts are positive, negative or null whether we are in quasi static regime (wt<<1) or dynamic frequencies regime (wt>>1). By the way, the phase of these recombination velocities can be:

- **Null:** There is no storage of the photogenerated carriers in solar cell interfaces. So, recombination of photogenerated carriers is analogue to joules effect noted in electrical resistance
- **Negative:** Some photogenerated carriers are stocked in solar cell interfaces. In this case, we consider the solar cell interfaces as a plan capacitor
- **Positive:** Recombination of photogenerated carriers is simulated as an inductive effect

The behaviour of the phase and the use of Bode and Nyquist diagrams (Lathi, 1973-1973) allow us to describe the intrinsic recombination velocities as electrical phenomenons. Also, considering carriers' recombination through the surface recombination velocity in semiconductors-electrodes (Searson *et al*., 1992; Hens and Gomes, 1999) in one hand and the impedance spectroscopy method (Chenvidhya *et al*., 2003; Suresh, 1995; Kumar *et al*., 2001; Dieng *et al*., 2007) in the other hand, electric equivalent models of intrinsic recombination velocities are proposed.

METHODOLOGY

Theory: We consider an n^+ - p - p^+ silicon solar cell whose structure can be schematized on Fig. 1.where d is the thickness of the emitter and Ho the total thickness of the solar cell

We use a one Dimensional (1D) mathematical model in which we neglect the grain boundaries recombination velocity. A constant magnetic field B is applied perpendicularly (Mbodji *et al*., 2009; Zouma *et al*., 2009) to the base of the solar cell.

The solar cell illumination generates pairs of electron-hole in the base. The evolution of excess minority (photogenerated) carriers is governed by the continuity equation given by:

$$\frac{\partial \delta_{n1}(x,t)}{\partial t} - D_n^* \frac{\partial^2 \delta_{n1}(x,t)}{\partial x^2} + \frac{\delta_{n1}(x,t)}{\tau_n} = G_1(x,t) \qquad (1)$$

where, $D_n^* \cdot \frac{D_n\left[\left(1+\tau_n^2(\omega_c^2+\omega^2)\right)+i\cdot\omega\cdot\tau_n\left(\tau_n^2(\omega_c^2+\omega^2)-1\right)\right]}{\left(1+\tau_n^2(\omega_c^2+\omega^2)\right)^2+4\cdot\omega^2\tau_n^2}$ is a complex diffusion coefficient dependent of magnetic field intensity and frequency modulation (Karlheinz, 1973;

Corresponding Author: Nd. Thiam, Laboratory of Semiconductors and Solar Energy, Physics Department, Faculty of Science andTechnology, University Cheikh Anta Diop, Dakar, Senegal

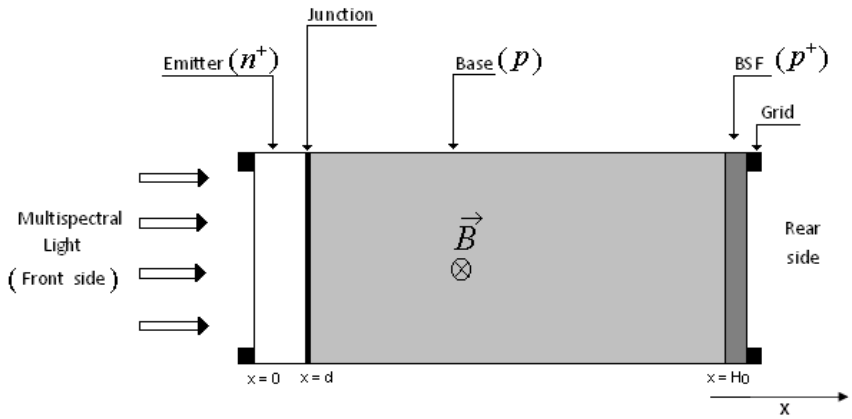

Fig. 1: An n^+-p-p^+ type of a silicon solar cell structure under applied magnetic field

SZE, 1981), $\omega_c = q\frac{B}{m_n}$ is cyclotron frequency (Cardona, 1969) of the electron on its orbit, m_n the effective mass of the electron supposed equal to his mass at the rest, q is the elementary charge of the electron, τ_n the excess minority carriers life time in the base; $\delta_{n1}(x,t)$ is the minority carrier density in the base and can be written as follow (Hollenhorst and Hasnain, 1995; Bousse *et al*., 1994; Ahmed and Garg, 1986):

$$\delta_{n1}(x,t) = \delta_{n1}(x)\exp(i\omega\cdot t) \tag{2}$$

where, $\delta_{n1}(x)$ the spatial part and $\exp(i\omega.t)$ temporal part of $\delta_{n1}(x,t)$, t is the time, $\omega = 2\pi f$ is the angular speed and f the frequency, $G_1(x,t)$ is the global generation rate given by Eq. (3) (Furlan and Amon, 1985):

$$G_1(x,t) = g_1(x)\exp(i\omega\cdot t) \tag{3}$$

$$\text{where, } g_1(x) = n\cdot\sum_{k=1}^{3} a_k\cdot\exp(-b_k x) \tag{4}$$

which is the spatial part of $G_1(x,t)$ and is the excess minority carriers generation at the position x of the base; n is solar number; a_k and b_k are coefficients deduced from modelling of the generation rate considered over all solar radiation spectrum under AM 1,5 (Mohammad, 1987). Substituting Eq. (2)-(3) in (1), we get:

$$\frac{\partial^2\delta_{n1}(x)}{\partial x^2} - \frac{1}{L_\omega^{*2}}\cdot\delta_{n1}(x) = -\frac{g_1(x)}{D_n^*} \tag{5}$$

where,

$$\frac{1}{L_\omega^{*2}} = \frac{1}{L_n^{*2}}\left(1 + i\omega\cdot\tau_n\right) \tag{6}$$

with L^*_n being the complex diffusion length of excess minority carriers in the base, function of magnetic field and frequency modulation, L^*_ω the generalize complex diffusion length (Mandelis, 1989).
The solution of Eq. (5) is given by:

$$\delta_{n1}(x,\omega) = A_1 ch\left(\frac{x}{L_\omega^*}\right) + B_1 sh\left(\frac{x}{L_\omega^*}\right) + \sum_{k=1}^{3}\beta_k\exp(-b_k x) \tag{7}$$

$$\text{with: } \beta_k = -\frac{n\cdot a_k\cdot L_\omega^{*2}}{D_n^*\left(b_k^2 L_\omega^{*2} - 1\right)}$$

$$\text{and } D_n^*\left(b_k^2 L_\omega^{*2} - 1\right) \neq 0 \tag{8}$$

where, the coefficients A_1 and B_1 are determinated by the following boundary conditions (Sissoko *et al*., 1992; Mialhe *et al*., 1991; Madougou *et al*., 2007b):

- At the junction:

$$D_n^*\cdot\left.\frac{\partial\delta_{n1}}{\partial x}\right|_{x=d} = Sf_1\cdot\delta_{n1}\big|_{x=d} \tag{9}$$

- At the rear side:

$$D_n^*\cdot\left.\frac{\partial\delta_{n1}}{\partial x}\right|_{x=H_o} = Sb_1\cdot\delta_{n1}\big|_{x=H_o} \tag{10}$$

where, Sf_1 and Sb_1 are respectively junction recombination velocity and back surface recombination velocity. The recombination velocity Sf_1 is the sum of the recombination velocity Sf(j) = $j.10^j$ cm/s due to the external charge that defines the solar cell operating point and the intrinsic recombination velocity Sfo1 that is an effective recombination velocity at the emitter-base interface.

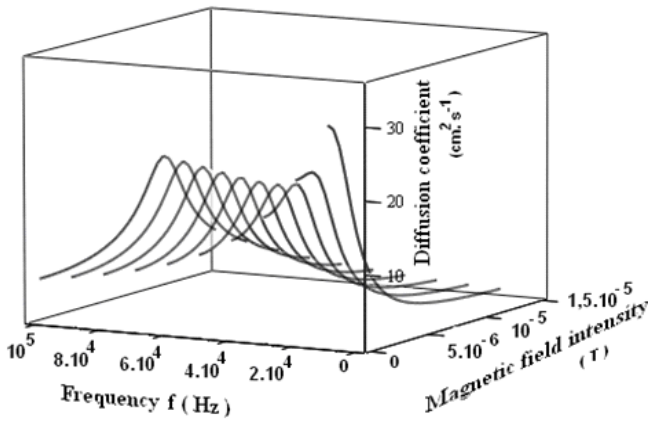

Fig. 2: Diffusion coefficient module versus frequency modulation f and magnetic field intensity B

Diffusion coefficient profile: The diffusion coefficient characterizing the minority carrier diffusion in solar cell base, is represented in 3 dimensions with regard to frequency modulation and applied magnetic field intensity on Fig. 2:

We observe on this figure that the module of diffusion coefficient decreases at a time with the increases of frequency modulation and magnetic field intensity. For a given values of magnetic field and frequency modulation, we observe that the diffusion coefficient increases slightly and presents a resonance pick. The frequency modulation corresponding to the diffusion coefficient pick, is called frequency of resonance. The reduction of the diffusion coefficient with the increase of the values of magnetic field and frequency modulation, modify the intrinsic properties of the solar cell by damaging them; this situation will affect the photocurrent density for example and then the intrinsic recombination velocity at the solar cell interfaces.

Photocurrent density profile: The density of photocurrent is obtained by the minority carriers' gradient at the junction and is given by the Eq. (11):

$$J_{ph1}(d, f, B, Sf) = qD_n^* \left.\frac{\partial \delta_{n1}}{\partial x}\right|_{x=d} \tag{11}$$

The module of the photocurrent density versus junction recombination velocity for different values of magnetic field and frequency modulation, is represented on Fig. 3:

We observe on this figure that the photocurrent density increases with regard to junction recombination velocity and presents three zones:

- The first zone corresponds to the solar cell operating in open circuit situation, where the photocurrent tends to zero ($Sfj<2.10^2$ cm/s);

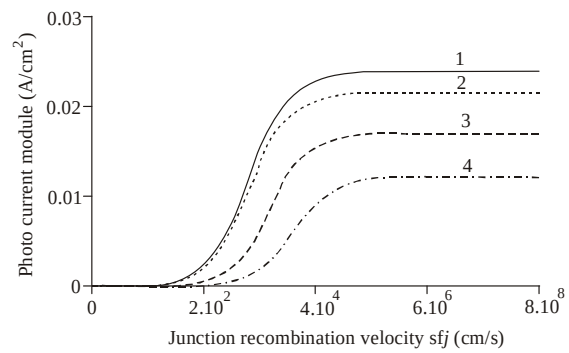

Fig. 3: Photocurrent density versus junction recombination velocity for a solar cell front side illumination
1º) B: 0 T; f: 0 Hz; 2º) B: 10^{-6} T; f: $2{,}804.10^4$ Hz; 3º) B: 10^{-5} T; f: $2{,}804.10^5$ Hz; 4º) B: 10^{-4} T; f: $2{,}804.10^6$ Hz

- The second zone for which $2.10^2<Sfj<5.10^5$ cm/s, corresponds to the solar cell variable operating point
- The third zone for which $Sfj>5.10^5$ cm/s corresponds to the solar cell operating in short circuit situation with the maximum values of photocurrent

The application of magnetic field leads to photocurrent density amplitude reduction and this situation is the consequence of minority carrier deviation by Lorentz strength due to the external magnetic field application.

Intrinsic recombination velocities: The profile of the photocurrent density in function of junction recombination velocity Sf and back surface recombination velocity Sb, present two stages. Thus, the expressions of the solar cell junction intrinsic recombination velocity Sfo1 and back surface recombination velocity Sbo1 are obtained below respectively from the Eq. (12) and (13) (Sissoko *et al*., 1998; Barro *et al*., 2004; Diallo *et al*., 2008):

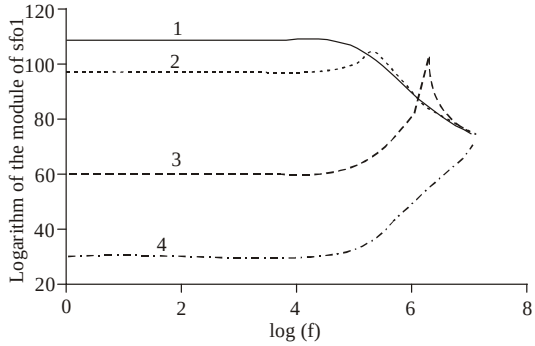

(a)

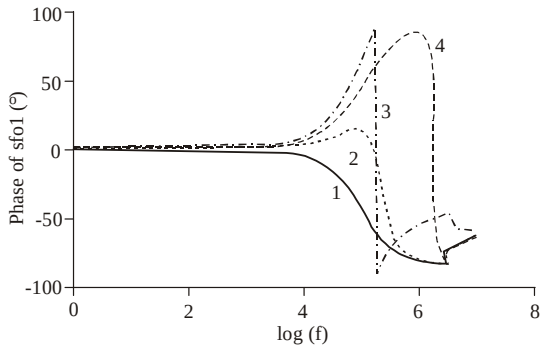

(b)

Fig. 4: Log (Sfo1) and its phase versus log (f)
1°) B: 0 T; 2°) B: 10^{-6} T; 3°) B: 10^{-5} T; 4°) B: 10^{-4} T

$$\left.\frac{\partial J_{ph1}(d, f, B, Sf)}{\partial Sb_1}\right|_{Sb_1 \succ 3.10^3 cm \cdot S^{-1}} = 0 \quad (12)$$

$$\left.\frac{\partial J_{Ph1}(d, f, B, Sf)}{\partial Sf_1}\right|_{Sf_1 \succ 5.10^5 cm.S^{-1}} = 0 \quad (13)$$

where,

$$Sfo1 = \sum_{k=1}^{3} \frac{D_n^*}{L_\omega^*} \frac{\left[b_k L_\omega^* \left(e^{-b_k H_o} ch\left(\frac{H}{L_\omega^*}\right) - e^{-b_k d} \right) + e^{-b_k Ho} Sh\left(\frac{H}{L_\omega^*}\right) \right]}{\left[e^{-b_k d} - e^{-b_k Ho} Ch\left(\frac{H}{L_\omega^*}\right) - b_k L_\omega^{*\,-b_k Ho} Sh\left(\frac{H}{L_\omega^*}\right) \right]} \quad (14)$$

and

$$Sfo1 = \sum_{k=1}^{3} \frac{D_n^*}{L_\omega^*} \frac{\left[b_k L_\omega^* \left(e^{-b_k d_o} ch\left(\frac{H}{L_\omega^*}\right) - e^{-b_k dHo} \right) - e^{-b_k d} Sh\left(\frac{H}{L_\omega^*}\right) \right]}{\left[e^{-b_k d} Ch\left(\frac{H}{L_\omega^*}\right) - e^{-b_k Ho} - b_k L_\omega^* e^{-b_k d} Sh\left(\frac{H}{L_\omega^*}\right) \right]} \quad (15)$$

The two expressions of the intrinsic recombination velocities are complex and we study their profiles for different values of magnetic field by using Bode and Nyquist diagrams.

Bode diagram of intrinsic recombination velocity:

Junction intrinsic recombination velocity Sfo1: We observe respectively on Fig. 4a and b, the logarithm of junction intrinsic recombination velocity module and its phase (define as the ratio of the imaginary part and the real part of the recombination velocity Sfo1). These curves are represented according to the logarithm of the modulation frequency for different values of magnetic field:

On Fig. 4a, in the interval of frequency [1Hz; 3.3 10^4 Hz], that means in quasi static's regime, the junction intrinsic recombination velocity module is independent of modulation frequency. When one applies magnetic field, we observe that the amplitude of the junction recombination velocity module decreases. Indeed, the application of magnetic field creates the magnetic strengths that act on the electrons by deviating them of their initial trajectory. It entails a slowing of the electrons that move to the junction and increases their probability of recombination in base volume.

In the interval [3.3 10^4 Hz; 10^8 Hz] that corresponds to the frequency dynamic regime, the module of the junction recombination velocity presents different variations:

- For a null value of applied magnetic field (curve 1), the module of the junction recombination velocity decreases with the increase of the modulation frequency.
- When we apply a magnetic field, we observe that junction recombination velocity module increases and this increase is bounded to the phenomenon of resonance gotten when the frequency of modulation is equal to the cyclotron frequency: there is much minority carrier recombination at the emitter-base interface. For modulation frequencies more than the frequency of resonance, the junction recombination velocity decreases.

The frequency 3.3 10^4 Hz called cut of frequency (Honma and Munakata, 1987), permits to determine the effective life time of minority carrier in the base of the solar cell. One observes on Fig. 4b that in quasi static's regime, junction recombination velocity phase is null with or without applied magnetic field. On the other hand, in frequency dynamic regime, one notes that:

- Without applied magnetic field, the phase is negative. There is minority carrier storage at the junction, that makes appear the capacity effect of the junction recombination velocity (Fig. 4a, curve 1),
- If we apply a magnetic field the phase becomes positive for frequencies lower or equal to the

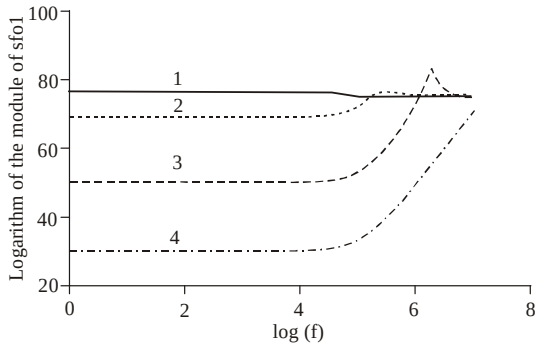

(a)

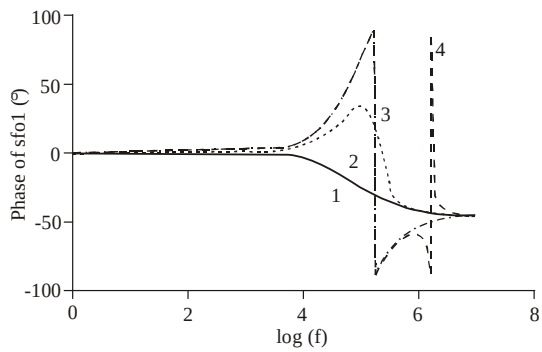

(b)

Fig. 5: Log (Sbo1) and its phase versus log (f)
1º) B: 0 T; 2º) B: 10^{-6} T; 3º) B: 10^{-5} T; 4º) B: 10^{-4} T

frequency of resonance, that point out the inductive effect of the junction intrinsic recombination velocity. On the other hand, for frequencies superior to the frequency of resonance, the phase becomes negative translating again the capacity effect of junction recombination velocity.

Back surface intrinsic recombination velocity Sbo1: We observe respectively on Fig. 5a and b, the logarithm of back surface intrinsic recombination velocity module and its phase. These curves are represented according to the logarithm of the modulation frequency for different values of magnetic field:

One observes on the Fig. 5a and b that the variations of the back surface intrinsic recombination velocity module and its phase in function of the logarithm of the modulation frequency, are identical to those presented by the Fig. 4a and b.

It appear from Fig. 4a and 5a, that the application of the magnetic field improves the emitter-base and base-rear contact interfaces in quasi static's regime. On the other hand, in frequency dynamic regime, these interfaces are real excess minority carrier's recombination centers, that corresponds to the behaviour of ohmic solar cell.

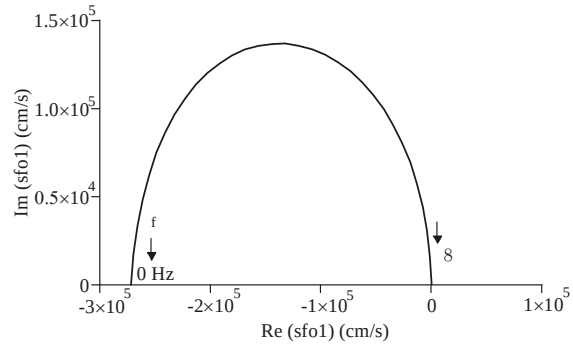

(a)

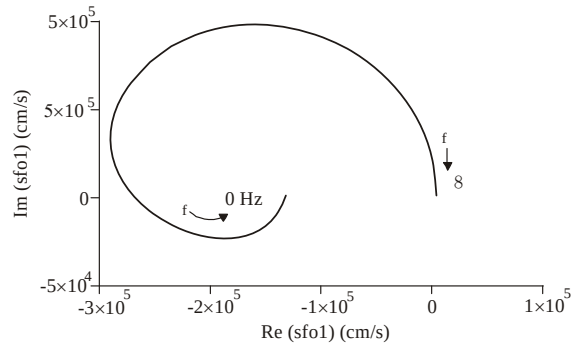

(b)

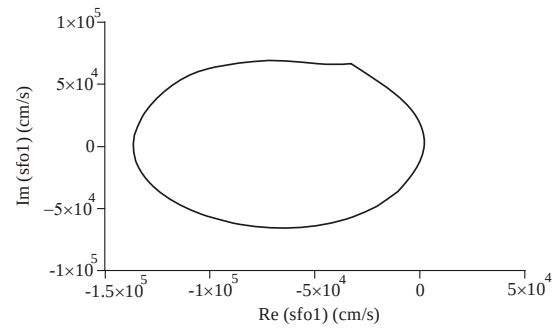

(c)

Fig. 6: Im (Sfo1) versus Re (Sfo1) a) B: 0 T; b) B: 10^{-6} T; c) B: 10^{-5} T

Nyquist of intrinsic recombination velocity:

Junction intrinsic recombination velocity Sfo1: The Fig. 6a, b and c illustrate the imaginary part of the junction intrinsic recombination velocity variation according to its real part, for different values of magnetic field.

One observes on Fig. 6a, without applied magnetic field, that the curve of intrinsic junction recombination velocity imaginary part variation according to its real part is a semi-circle. On the other hand, one observes on the Fig. 6b and c that with the application of the magnetic

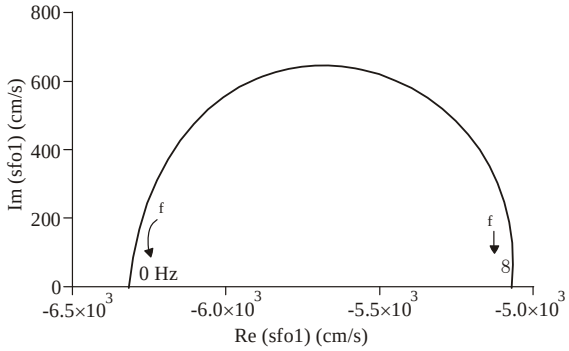

(a)

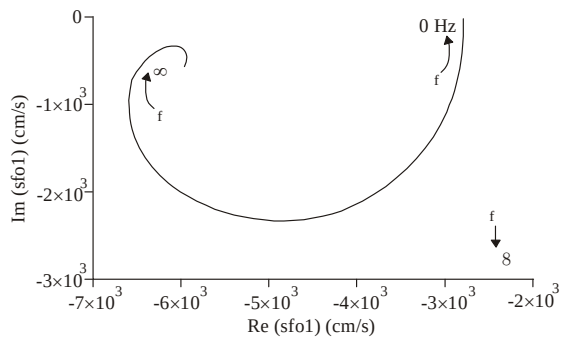

(b)

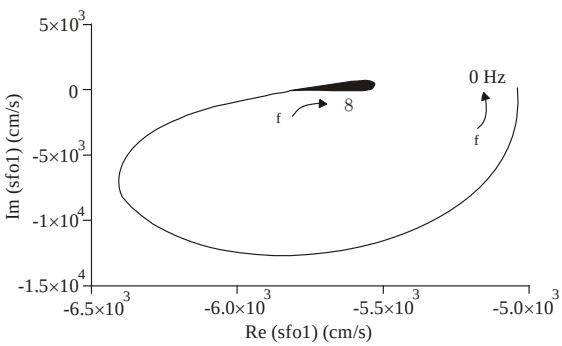

(c)

Fig. 7: Im (Sbo1) versus Re (Sbo1)
a) B: 0 T; b) B: 10^{-6} T; c) B: 10^{-5} T

field, the curve of variation of junction recombination velocity imaginary part according to the real part present respectively the shapes of spiral and circle.

One observes on the Fig. 6a, without applied magnetic field, the imaginary part of the intrinsic junction recombination velocity stretches toward zero when the modulation frequencies *f* stretch toward zero and toward the infinity. In this range of frequency, the imaginary part is positive and the real part is negative. So the phase will always be negative and it confirms the capacity effect of Sfo1 observed above.

When we apply a magnetic field, one observes on the curves 6-b and 6-c that, for frequencies *f* included between zero and to the frequency of resonance, imaginary and real parts values are nulls. In this domain of frequency we will have the positives phases that characterize Sfo1 inductive effect observed on the Fig. 4b therefore. Beyond the resonance frequency, it is again the capacity effect of the intrinsic junction recombination velocity that appears.

Back surface intrinsic recombination velocity Sbo1: The Fig. 7a, b and c illustrate the imaginary part of the back surface intrinsic recombination velocity variation according to its real part, for different values of magnetic field.

The interpretation of the curves of Fig. 7 let appear that, as the intrinsic junction recombination velocity, the capacity effect of the intrinsic back surface recombination velocity is predominant in magnetic field absence (Fig. 7a). On the other hand, when we apply magnetic field the inductive effect appears for included frequencies between zero and resonance frequency. Beyond resonance frequency, it is again the capacity effect that appears (Fig. 7b and c).

Electric equivalent models of intrinsic recombination velocities: In this paragraph, we propose electric equivalent models of the intrinsic recombination velocities through the results obtained from Bode and Nyquist diagrams.

Junction intrinsic recombination velocity Sfo1: The storage, the losses and the reduction of the recombination of excess minority carriers at the emitter-base interface, can be respectively electrically modelized by a capacity, a loss resistance and a series resistance. In the case of magnetic field absence, the curve of variation of the imaginary part of the intrinsic junction recombination velocity according to its real part can be translated in an electric diagram as proposed on the Fig. 8.

In this model, *C* characterizes the capacity effect of the intrinsic junction recombination velocity (negative phase); R_p is a parallel resistance that characterizes carrier's losses in the emitter-base interface and *R* a resistance characterizing the minority carrier slowing in the emitter-base interface.

When one applies a magnetic field, in addition to the electric parameters above it appears an inductive effect (positive phase) of the intrinsic junction recombination velocity that we characterize by an inductance *L*. The electric diagram of the junction recombination velocity is given by the Fig. 9.

In this model, the inductance *L* characterizes the capacity of the emitter-base interface to recombine the excess minority carriers.

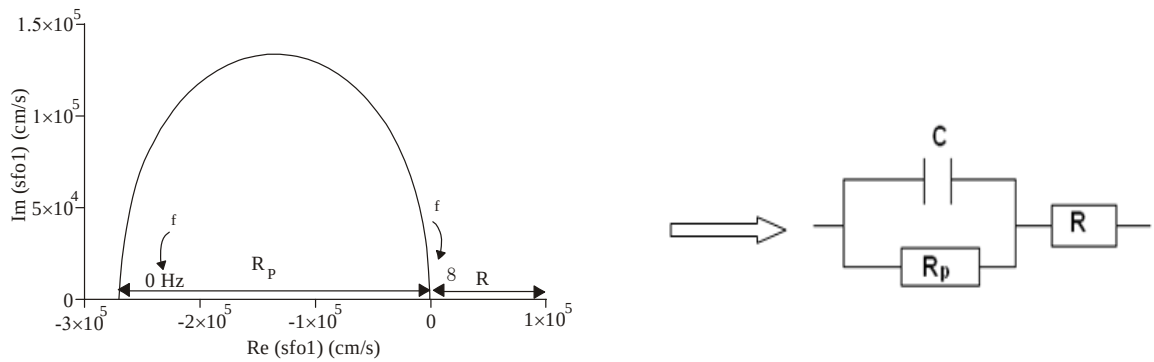

(a) (b)

Fig. 8: Electric equivalent circuit of Sfo1 without applied magnetic field

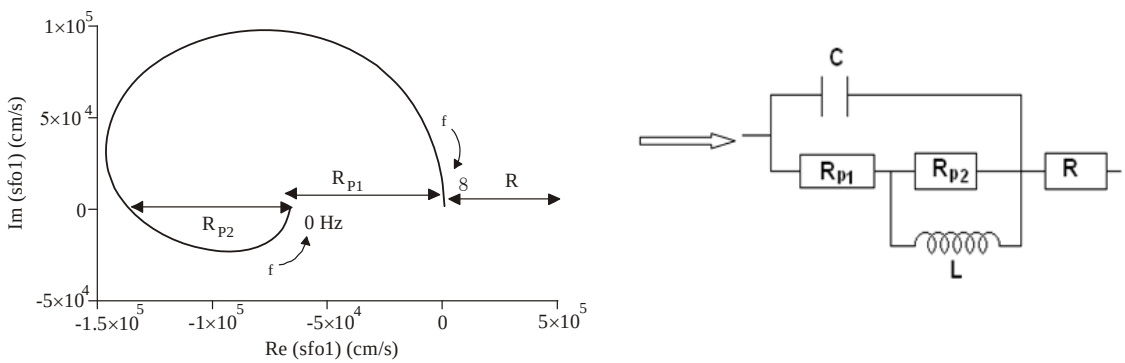

(a) (b)

Fig. 9: Electric equivalent circuit of Sfo1 with applied magnetic field

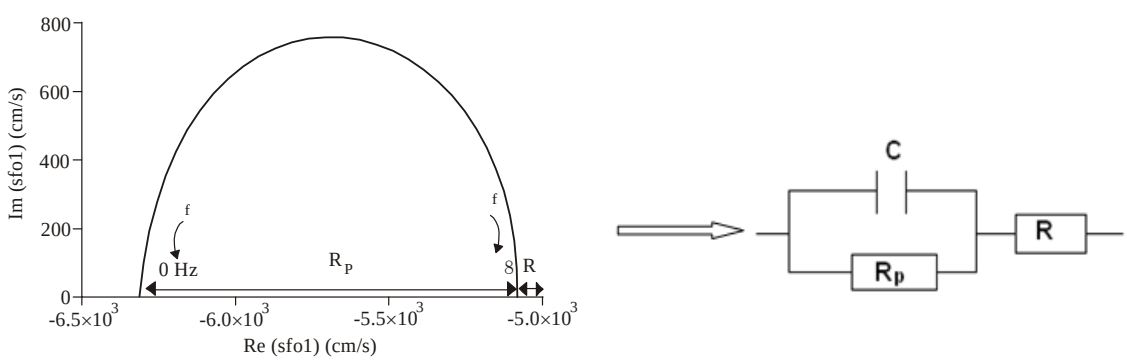

(a) (b)

Fig. 10: Electric equivalent circuit of Sbo1 without applied magnetic field

Back surface intrinsic recombination velocity Sbo1: The rear zone of the solar cell constitutes a zone of strong recombination of the excess minority carriers. We also intend an electric model of the intrinsic back surface recombination velocity. Thus, when we don't apply a magnetic field, the electric circuit is given by the Fig. 10.

C is a capacity of recombination in the rear zone; R_p is a parallel carriers flight resistance at the base-rear

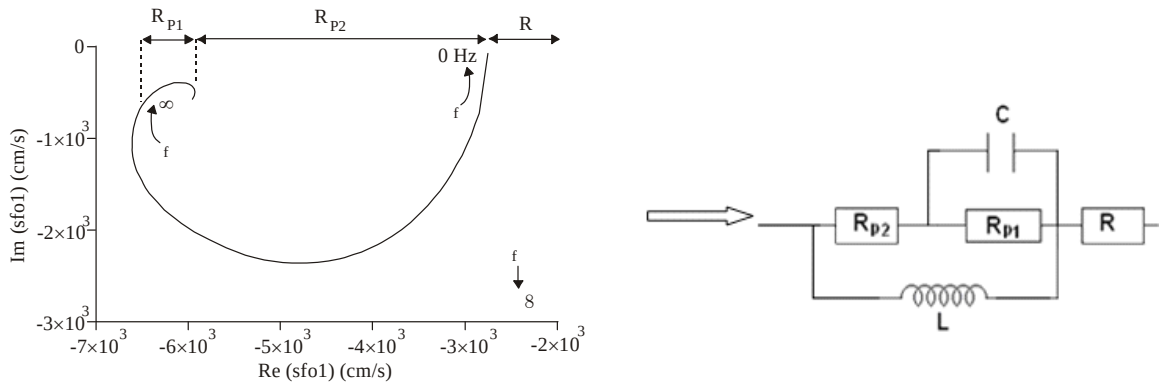

(a) (b)

Fig. 11: Electric equivalent circuit of Sbo1 without applied magnetic field

contact interface and *R* a resistance that materializes excess minority carriers slowing at this interface.

While applying a magnetic field, an electric diagram holding count of the inductance L (positive phase) is given in the Fig. 11.

The inductance *L* characterizes the capacity of the base-rear contact interface to recombine the excess minority carriers.

RESULTS AND DISCUSSION

In this paragraph, we determine the electric parameters of different electric circuit proposed for intrinsic recombination velocities Sfo1 and Sbo1. The electric parameter determination is made on the basis of approximations in the domain of frequency modulation.

Intrinsic junction recombination velocity Sfo1: The values of the electric parameters of the equivalent circuit of Sfo1, can be determined as follows:

- Without magnetic field:
  - Rp is the diameter of the semi-circle.
  - R can be determined by making stretch the *f* frequency toward zero or toward the infinity: when *f* stretches toward the infinity, Im (Sfo1) = 0, Re (Sfo1) = R; when *f* stretches toward zero, Im (Sfo1) = 0 and Re (Sfo1) = Rp+R.
  - from the constant of life time $t = R_p.C$ that is equal to the middle excess minority carrier life time, we can deduce the value of the capacity C.
- If we applied a magnetic field, the resistances R_{P2} and R_{P1} are determined as follow:
  - While making stretch *f* toward the infinity, one determines the value of R: when *f* stretches toward the infinity, Im (Sfo1) = 0 and Re (Sfo1) = R.
  - R_{p1} is determined while making stretch *f* toward zero: when *f* stretches toward zero, Im (Sfo1) = 0 and Re (Sfo1) = R_{p1}+R.
  - R_{p2} is deduced from resonance frequency: when *f* = *fo*, Im (Sfo1) = 0 and Re (Sfo1) = R_{p1}+R_{p2}+R.
  - In the same way, R_{p2} can be determined from the first semi-circle of which it is the diameter. In this interval of frequency where the inductive effect of the recombination velocity Sfo1 is more important than it capacity effect, the tracing of Im (Sfo1) according to the frequency is a linear curve of which the slope is the inductance L.
  - The second semi-circle whose diameter equal R_{P1}+R_{P2}, permits the determination of R_{p1}. While using the relation $\tau = (RP_1 + RP_2)C$, one calculates the value of *C*.

The electric parameters of Sfo1 are given by Table 1:

It appears on this table that even for a small variation of the applied magnetic field, the *R* resistance is constant but the capacity of recombination *C* increases.

Intrinsic back surface recombination velocity Sbo1: The values of the electric parameters of the equivalent circuit of Sbo1, can be determined as follows:

- **Without magnetic field:**
- R_p is the diameter of the semi-circle.
- R can be determined by making stretch the *f* frequency toward zero or toward the infinity: when *f* stretches toward the infinity, Im (Sbo1) = 0, Re (Sbo1) = R; when *f* stretches toward zero, Im (Sbo1) = 0 and Re (Sbo1) = R_p+R.
- From the constant of life time $t = R_p.C$ that is equal to the middle excess minority carrier life time, we can deduce the value of the capacity C.

Table 1: Values of the electric parameters for Sfo1

Magnetic field intensity B (tesla)	R_p	R_{p1}	R_{p2}	R	C	L
0	270 KΩ	X	X	50 KΩ	37 pF	X
10^{-6}	X	67 KΩ	69 KΩ	50 KΩ	73 pF	5 µH

Table 2: Values of the electric parameters for Sbo1

Magnétic field intensity B (tesla)	R_p	R_{p1}	R_{p2}	R	C	L
0	1.25 KΩ	X	X	5 KΩ	8 nF	X
10^{-6}	X4	95 Ω	3.7 KΩ	3 KΩ	20 nF	6 µH

- If we apply a magnetic field, the resistances R_{P2} and R_{P1} are determined as follow:
- While making stretch *f* toward zero, one determines the value of R: when *f* stretches toward the zero, Im (Sbo1) = 0 and Re (Sbo1) = R.
- R_{p2} determine while making stretch *f* the infinity: when *f* stretches toward the infinity, Re (Sbo1) = R_{p2}+R.
- The second semi-circle whose diameter equal R_{P1}, permits the determination of R_{p1}
- R_{p2} can be also deduced from resonance frequency: when $f = fo$, Im (Sbo1) = 0 and Re (Sbo1) = $R_{p1}+R_{p2}+R$. The first semi-circle permits the deduction of ($R_{p1}+R_{p2}$) which is its diameter. In this interval of frequency where the inductive effect of the recombination velocity Sbo1 is more important than it capacity effect, the tracing of Im (Sbo1) according to the frequency is a linear curve of which the slope is the inductance L.
- From the relation $t = R_{p1}.C$, we can deduce the value of the capacity *C*.

The electric parameters of Sbo1 are given by Table 2:

One observes on Table 2 that, in the electric model of recombination velocity Sbo1, the resistance R and the recombination capacity are sensitive to the weak values of the applied magnetic field.

According to the Table 1 and 2, it appears that the parallel resistances corresponding to the recombination velocity Sbo1 are lower to those of recombination velocity Sfo1. This result is the consequence of the fact that the minority carrier recombination is more important at the base-rear contact interface than at the emitter-base interface. There few minority carriers stocked in rear zone compared to the emitter-base interface. This phenomenon is responsible of the weak values of the capacity C at the base-rear contact interface comparatively to those of the emitter-base interface. For the same reasons one observes that the inductance L of the base-rear contact interface is superior to the one of the emitter-base interface.

CONCLUSION

A theoretical study made in the base of a silicon solar cell under multispectral light illumination in frequency modulation and under external magnetic field effect, has been presented. The expressions of the intrinsic junction and back surface recombination velocities of the solar cell are determined. These recombination velocities were studied through Bode and Nyquist diagrams. The study of these recombination velocities shows that with the application of the magnetic field, the interfaces emitter-base and base-rear contact are improve in quasi static regime. In frequency dynamic regime, the increase of the recombination velocities causes excess minority carriers losses at the interfaces, that also explains the bad quality of the solar cell in high frequency. Taking account of Bode and Nyquist diagrams, equivalent electric models that illustrate the evolution of the intrinsic recombination velocities Sfo1 and Sbo1, are proposed.

REFERENCES

Ahmed, F. and S. Garg, 1986. Simultaneous determination of diffusion length, lifetime and diffusion constant of minority carriers using a modulated bea. International Centre for Theoretical Physics, Trieste, Italy Internal Report.

Barro, F.I., S. MBodji, A.L. NDiaye, I. Zerbo, S. Madougou, F. Zougmore and G. Sissoko, 2004. Bulk and surface parameters determination by a transient study of bifacial silicon solar cell under constant white bias light. Proceedings of the 19th European Photovoltaic Solar Energy Conference and Exhibition, pp: 262-265.

Bousse, L., S. Mostarshed, D. Hafeman, M. Sartore, M. Adami, *et al*., 1994. Investigation of carrier transport through silicon wafers by photocurrent measurements. J. Appl. Phys., 75(8): 4000-4008.

Cardona, M., 1969. Modulation Spectroscopy, Solid State Physics. Suppl. 11.

Chenvidhya, D., K. Kirtikara and C. Jivacate, 2003. Solar Energy Materials and Solar Cells 80459-464.

Daniel, L.M., H. Jeong-Mo and B.C. Robert, 1988. IEEE Trans. Electr. Dev., ED-35(1): 70-78.

Diallo, H.L., A.S. Maiga, A. Wereme and G. Sissoko, 2008. New approach of both junction and back surface recombination velocities in a 3D modeling study of a polycrystalline silicon solar cell. Eur. Phys. J. Appl. Phys., 42: 203-211.

Dieng, A., L. Ould Habiboulahy, A.S. Maiga, A. Diao and G. Sissoko, 2007. Impedance spectroscopy method applied to electrical parameters determination on bifacial silicon solar cell under magnetic field. J. Sci., 7(3): 48-52.

Furlan, J. and S. Amon, 1985. Approximation of the carrier generation rate in illuminated silicon. Solid State Electr., 28(12): 1241-1243.

Honma, N. and C. Munakata, 1987. Sample thickness dependence of minority carrier lifetimes measured using an ac photovoltaic method. Jap. J. Appl. Phys., 26(12): 2033-203.

Hens, Z. and W.P. Gomes, 1999. The Electrochemical impedance of one-equivalent electrode processes at dark semiconductor/redox electrodes involving charge transfer through surface states.2. The n-GaAs/Fe^{3+} system as an experimental example. J. Phys. Chem. B, 103(1): 130-138.

Hollenhorst, J.N. and G. Hasnain, 1995. Frequency dependent whole diffusion in InGaAs double heterostructure. Appl. Phys. Lett., 67(15): 2203-2205.

Hübner, A., A.G. Aberle and R. Hezel, 2001. 20% efficient bifacial silicon solar cells.14th European PVSEC, pp: 1796-1798.

Karlheinz, S., 1973. Semiconductor Physics. Springer-Verlag/Wien, New York, Print in Austria by B. Müller, pp: 269. ISBN: 0-387-81186-9.

Kumar, R.A., M.S. Suresh and J. Nagaraju, 2001. Measurement of AC parameters for gallium arsenide (GaAs/Ge) solar cell by impedance spectroscopy. IEEE T. Electr. Dev., 48(9): 2177-2179.

Lathi, B.P., 1973-1974. Signals, Systems and Controls. Intext Educational Publisher, New York.

Madougou, S., F. Made, M.S. Boukary and G. Sissoko, 2007b. Recombination parameters determination by using Internal Quantum Efficiency (IQE) data of bifacial silicon solar cells advanced materials research. Trans. Tech. Pub. Inc., 18-19: 313-324.

Mandelis, A., 1989. Coupled ac. Photocurrent and photothermal reflectance response theory of semiconducting p-n junctions. J. Appl. Phys., 66(11): 5572-5583.

Mbodji, S., A.S. Maiga, M. Dieng, A. Wereme and G. Sissoko, 2009. Renoval Charge technical applied to a bifacial solar cell under constant magnetic field. Global J. Pure Appl. Sci., 15(1,): 125-132.

Mialhe, P., J.M. Salagnon, F. Pelanchon, G. Sissoko and M. Kane, 1991. Lifetime and surface recombination determination Proceeding of 10th European Photovoltaic Solar Energy Conference and Exhibition, pp: 36-38.

Mohammad, S.N., 1987. An alternative method for the performance analysis of silicon solar cells. J. Appl. Phys., 61(2): 767-772.Searson, P.C., D.D. Macdonal and M.P. Laurence, 1992. Frequency domain analysis of photoprocesses at illuminated semiconductor electrodes by transient transformation. J. Electrochem. Soc., 139(9): 2538-2543.

Sissoko, G., E. Nanéma, A. Corréa, P.M. Biteye, M. Adj and A.L. N'Diaye, 1998. Silicon Solar cell recombination parameters determination using the illuminated I-V characteristic. World Renewable Energy Congress, pp: 1847-1851.

Sissoko, G., S. Sivoththanam, M. Rodot and P. Mialhe, 1992. Constant Illumination-Induced Open Circuit Voltage Decay (CIOCVD) method, as applied to high efficiency Si Solar cells for bulk and back surface characterization. 11th European Photovoltaic Solar Energy Conference and Exhibition, Poster 1B, 12-16, Montreux, Switzerland, pp: 352-354.

Suresh, M.S., 1995. Measurement of solar cell parameters using impedance spectroscopy. Sol. Energ. Mater. Sol. Cell., 43: 21-28.

SZE, S.M., 1981. Physics of Semiconductor Devices. John Wiley and Sons, New York.

Wang, A., J. Zhao and M.A. Green, 1990. 24% efficient silicon solar cells. Appl. Phys. Lett., 57: 602-604.

Zouma, B., A.S. Maiga, M. Dieng, F. Zougmore and G. Sissoko, 2009. 3rd approach of spectral response for a bifacial silicon solar cell under a constant magnetic field. Global J. Pure Appl. Sci., 15(1): 117-124.